Pure Appl. Chem., Vol. 83, No. 1, pp. 127–139, 2011.
doi:10.1351/PAC-CON-10-08-23

Recent design strategies for polymer solar cell materials*

David Bilby[1], Bong Gi Kim[2], and Jinsang Kim[1,2,3,4,‡]

[1]Department of Materials Science and Engineering, University of Michigan, Ann Arbor, MI, USA; [2]Department of Macromolecular Science and Engineering, University of Michigan, Ann Arbor, MI, USA; [3]Department of Chemical Engineering, University of Michigan, Ann Arbor, MI, USA; [4]Department of Biomedical Engineering, University of Michigan, Ann Arbor, MI, USA

Abstract: Recent design tools for tuning the properties of conjugated polymers for efficient polymer solar cells (PSCs) are briefly reviewed. Based on limitations in the solar-to-electric energy conversion process imposed by material properties, recent research has focused on lowering the highest occupied molecular orbital (HOMO) level, reducing the bandgap, and controlling the molecular conformation and donor–acceptor phase separation. Additionally, the stability of PSCs can be improved through molecular design. Finally, a few less-conventional material design strategies for device improvement through polymer–polymer blends and triplet utilization are introduced. Molecular design has been an invaluable tool in controlling these material properties.

Keywords: conjugated polymers; design review; molecular design; organic electronics; organic solar cells.

INTRODUCTION AND BACKGROUND

Organic photovoltaics have commanded quite an interest in the renewable energy devices research community [1]. These devices will take advantage of the vast resource that is sunlight as well as relatively inexpensive processing routes. Polymer solar cells (PSCs), due to their solution processability, show promise to eventually be cost competitive with conventional fossil fuel-based electricity generation technologies. Roll-to-roll processing enables large-scale, morphology-optimized production of these devices [2–5]. Thus, increasing device efficiency and lifetime through device and polymer design remain the primary obstacles to cost competitiveness [3–5]. However, with record power conversion efficiencies (PCEs) reaching 8.13 % and lifetimes greater than 1 year, these devices are on track to become economically viable [6,7].

A brief explanation of the operational physics of PSCs provides the foundation for device improvement through molecular design. First, a photon, of sufficient energy to overcome the highest occupied (HOMO) to lowest unoccupied (LUMO) molecular orbital energy level bandgap of the conjugated polymer, is absorbed. This creates a charge-neutral, tightly bound electron hole pair known as an exciton. In order to extract this energy, the exciton must diffuse to an interface with an electron-accepting material (typically, phenyl C_{61} butyric acid methyl ester (PCBM)) where charge transfer rap-

Pure Appl. Chem.* **83, 1–252 (2011). A collection of invited, peer-reviewed articles by former winners of the IUPAC Prize for Young Chemists, in celebration of the International Year of Chemistry 2011.
‡Corresponding author: Tel.: (734) 936-4681; Fax: (734) 763-4788; E-mail: jinsang@umich.edu

idly takes place, splitting the exciton into a hole and an electron [8–10]. The separated charges are then conducted to their respective electrodes to power an external circuit.

The specifics of the power conversion physics combine with material properties to impose constraints on the fabrication and performance of the devices. For instance, the exciton diffusion length in conjugated polymers is typically very short; in a very common electron donor polymer, poly(3-hexylthiophene) (P3HT, Fig. 1a), the exciton diffusion length is about 8.5 nm [9,11]. This means that in a

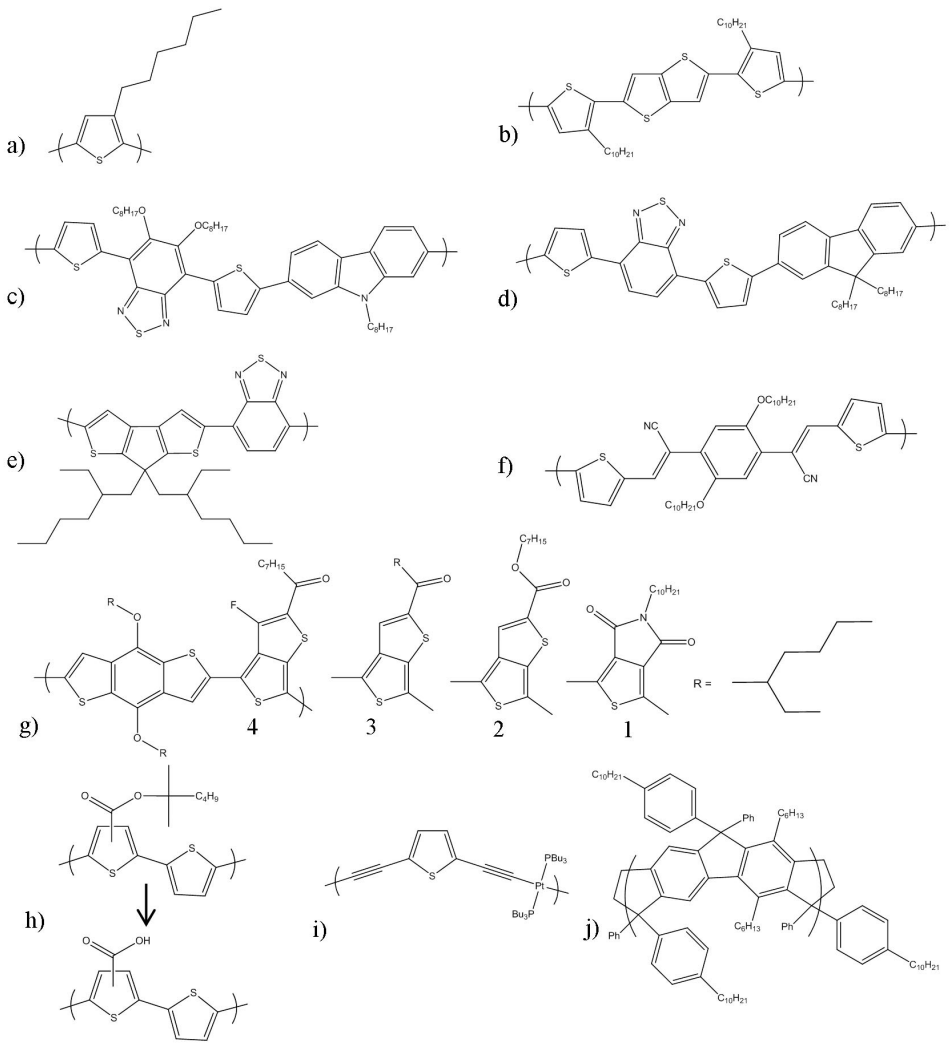

Fig. 1 Chemical structures of interesting conjugated polymers for PSCs. (a) P3HT, (b) high hole mobility PBTTT exhibits a fused ring thienothiophene and control over side-chain spacing and length [30], (c) by incorporating an electron-donating carbazole and an electron-withdrawing benzothiadiazole, this is a low-bandgap polymer [26], (d) low-bandgap polymer exhibiting a fluorene donor and benzothiadiazole acceptor [31], (e) low-bandgap polymer with a strong donor (cyclopentadithiophene) and benzothiadiazole as an acceptor [32], (f) electron-withdrawing cyano pendants lower the HOMO of this polymer [33], (g) increasing the strength of electron-withdrawing comonomers (in the order 2,3,4,1) contribute to a lower HOMO in combination with electron-donating benzoditihophene [34,35], (h) thermally cleavable side groups allow for thermal stability of the PSC morphology [36,37], (i) a novel thiophene acetylide polymer with Pt in the backbone that promotes triplet generation [38], (j) a novel ladder-type poly(*p*-phenylene) with 120–200 ppm covalently bound Pd promotes triplet generation [39].

device that is thick enough to absorb most of the incident sunlight (about 240 nm thick) most of the excitons will recombine rather than separate into useful charges [12]. This deficiency is overcome by using a bulk-heterojunction device morphology; interpenetrating domains of the electron acceptor and donor materials provide nearby charge separation interfaces wherever an exciton may form [13]. Additionally, charge carrier mobilities in polymer materials are quite low, typically ranging from 10^{-6} to 10^{-1} cm^2 V^{-1} s^{-1}, limiting the distance charges can travel before succumbing to recombination (and therefore limiting the overall device thickness) [14–16]. Thus, compromises are made with regards to device thickness in order to optimize both device current density and absorption [16].

Innovative molecular design seeks to take advantage of the operational physics of the devices in order to overcome material limitations in PSCs. This allows for enhanced open-circuit voltage (V_{oc}), short-circuit current density (J_{sc}), and fill factor leading to an increased PCE [17–21]. The following discussion will present many design routes which have been taken to tune morphology, polymer packing, and molecular orbital energy levels, among other things, of the electron-donating conjugated polymer materials. The influence of these design changes on the PSC performance via the aforementioned operational physics will also be discussed. These ideas represent some basic molecular design methods to improve PSCs, and they provide an underpinning for future PSC material development.

DESIGN RULES FOR ELECTRON DONOR MATERIALS

Inter- and intramolecular conformation control

The energy transfer and transport characteristics of conjugated polymers depend greatly on their physical conformation [22,23]. The spacing and orientation between two chromophores (or other energy transfer systems) can dictate the extent and type (long-range Forster via dipoles or short-range Dexter via diffusion/contact) of energy transfer that occurs. Similarly, energy transport within a single chromophore system is influenced by molecular planarity and packing. Because of these effects, much effort has been given to control the conformation of conjugated polymers for PSCs [18,21,24–30].

One major goal of polymer conformation control is to increase the chain planarity. Highly planar chains extend the effective conjugation length of the polymer. This improves absorption by red-shifting the bandgap energy, and it improves exciton and charge transport by further delocalizing electrons and excited states while reducing the population of carrier trapping sites. Strategies to increase polymer planarity have previously involved designing tight-packing, fairly crystalline materials [24,29,30]. Although the crystallinity is typically enhanced by post-processing annealing steps, design of the polymer can improve this characteristic. For instance, by controlling the regioregularity, spacing, and size (length and bulkiness) of the solubilizing side-chains, one can create a material with a high tendency to tightly pack and π–π stack its conjugated backbone [24]. Through these methods (Fig. 1b), charge carrier mobilities of 0.6 cm^2 V^{-1} s^{-1} have been achieved [30].

More recently, design of conjugated polymers with a high degree of backbone planarity has focused on the moieties in the backbone itself. Besides the aforementioned sterics of side-chain interactions, bulky conjugated segments of the polymer backbone can also inhibit planarity. For instance, bonds to thiophenes are potentially more planar than bonds to benzene because the five-membered ring is physically smaller near the backbone linkage. This provides relatively less steric interference at the bond, thus allowing for a planar conjugated backbone. Alternately, some research groups are including a vinylene group along the backbone because it is very small and still maintains the conjugation [25]. Both of these routes reduce the steric interactions between conjugated backbone structures and reduce backbone twist relative to other, more bulky moieties.

The most popular and successful route to maintain conjugated polymer planarity is to use fused ring structures along the backbone. This removes most of the flexibility from relatively larger sections of the polymer because the ring structures are much more rigid than the (conjugated) "single" bonds that are conventionally used. Even in polymers with fairly bulky side-chains, the effect of the planar,

fused rings comes through. Because of these effects, many researchers have incorporated moieties with two- and three-ringed structures into polymers and have achieved PSC efficiencies greater than 4 % [18,21,26,27]. Finally, the two aforementioned methods, which involve control of sterics, are commonly implemented and balanced together with the fused ring method in order to optimize backbone planarity. Although many other routes for controlling molecular planarity exist (via secondary bonding interactions such as hydrogen bonding), these three are the primary ones used in PSCs to improve charge carrier and exciton transport [40–42].

Efficient PSCs should produce a large voltage in addition to a large current density. When characterizing a device, a potential is swept across it from the point of maximum current (J_{sc}) to the point of no current flow (V_{oc}). While losses in J_{sc} are primarily the result of poor transport (and can be reduced by improving polymer planarity), both V_{oc} and J_{sc} are influenced by intermolecular energy transfer. Current generation relies on efficient electron transfer from the donor to the acceptor molecule, however the converse of this, bimolecular recombination from the charge-transfer state, is detrimental to the V_{oc} [43,44].

As stated earlier, intermolecular spacing and conformation greatly influence energy transfer, thus, in an effort to reduce losses to the V_{oc} via bimolecular recombination, molecules are designed to control intermolecular spacing. For instance, in a small-molecule-based solar cell Perez et al. chose donor molecules with bulky pendant groups and showed that the V_{oc} losses were decreased [44]. The bulky pendant groups increased the spacing between donor and acceptor molecules and thus reduced the level of intermolecular recombination. Similarly, many donor polymers in PSCs with high V_{oc} and low V_{oc} losses utilize long or bulky side-chains like the 2-ethylhexyl group (Fig. 1g) [18,27,31,34,35,45–47].

As has been discussed, control over the inter- and intramolecular conformation of electron donor polymers is of great interest in optimizing PSCs. While careful design of the molecule can lead to tuned properties, some of these design changes follow naturally from each other. For instance, since conjugated polymers are rigid, they require side-chains for good solubility. When taking advantage of the enhanced planarity of fused conjugated rings, larger, bulky side-chains become necessary in order to obtain sufficient solubility. Thus, both the inter- and intramolecular energy transfer and transport character will be affected. Finally, although other forms of conformation-induced changes in energy transport and transfer exist (orientation, etc.), control over these through molecular design has not been explored in PSCs to the best of the authors' knowledge.

Electronic bandgap and absorption tuning

One simple requirement for an efficient PSC is effective utilization of the solar spectrum. Absorption of light is dependent on the conjugated polymer's bandgap energy; however, conventional conjugated polymers usually have wide bandgaps. For instance, the most widely studied polymer for PSCs, P3HT, has a bandgap energy around 1.9 eV. Since more than 52 % of the total solar irradiance is at energies below 1.77 eV, there has been much interest in tailoring/reducing the polymer bandgap to absorb more of the solar spectrum [48,49].

The primary way to increase absorption of the solar spectrum is to reduce the energy required to excite the electron donor conjugated polymer. The simplest scheme involves polymer planarity and packing: increasing the effective conjugation length can red-shift the absorption slightly (by about 0.3 to 0.6 eV) due to increased delocalization of the π-electrons [29]. This effect is primarily seen in the film state of the polymers relative to their solution-state absorption (especially in regioregular P3HT). More effective means of reducing the bandgap rely on chemical tuning [50]. By alternating electron-donating and -withdrawing moieties in the conjugated polymer's structure, one can reduce the bandgap (Figs. 1c–e, g, Fig. 2) [51]. This push–pull structure allows for absorption transitions not only by the polymers' individual moieties, but also in between them because of an appreciable difference in their energy levels (Fig. 2, left). By setting up an internal donor–acceptor structure, the bandgap is reduced to that of the intramolecular charge-transfer absorption edge [51].

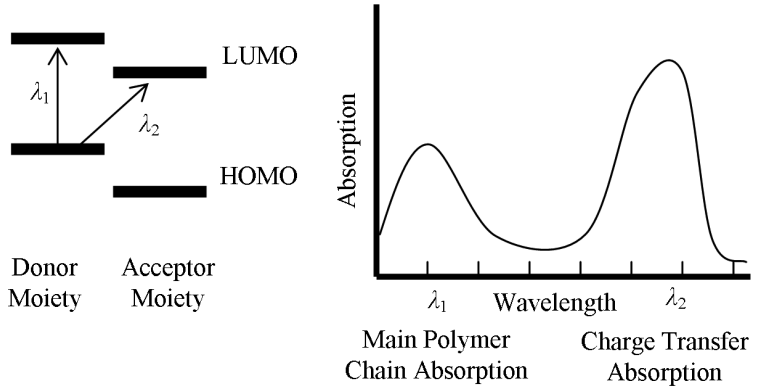

Fig. 2 Strategies for low bandgap-conjugated polymers: Intramolecular charge transfer. Alternating electron-donating and -withdrawing moieties can result in a reduced bandgap because the relatively blue absorption of the polymers main chain (λ_1) is augmented by a lower-energy charge-transfer (between the donor and acceptor moieties, λ_2) absorption.

Polymers containing alternating electron-donating and -withdrawing moieties, either along the main backbone chain or within side-chains, have tuned bandgaps [17,52]. For instance, by creating a copolymer of alternating benzodithiophene and thieno[3,4-c]pyrrole-4,6-dione units (Figs. 1g–1) Zou et al. were able to achieve a bandgap of about 1.8 eV [35]. Although the absorption edge is not very red-shifted relative to P3HT, the combination of the electron-donating benzodithiophene and electron-withdrawing thieno-pyrrole-dione units does lower the bandgap. Additionally, a bandgap of about 1.4 eV can be achieved with alternating 2,1,3-benzothiadiazole (strong acceptor) and cyclopentadithiophene (strong donor) units (Fig. 1e) [32]. These moieties are chosen based on the intramolecular conformation considerations discussed earlier as well as their relative donor or acceptor strength. Increasing the strength of a donor (by raising its HOMO) or acceptor (by lowering its LUMO), all else equal, will result in a reduced bandgap. Some common donor moieties include carbazole, fluorene, thiophene, and thienothiophene (in the polymers in Fig. 1). There are also many electron-withdrawing moieties (some candidates are in Fig. 3), but the most popular is 2,1,3-benzothiadiazole (in many polymers in Fig. 1) (more will be presented later about energy level tuning) [53]. Thus, by varying the donating and withdrawing strength of the constituent moieties, one can achieve a wide range of bandgaps.

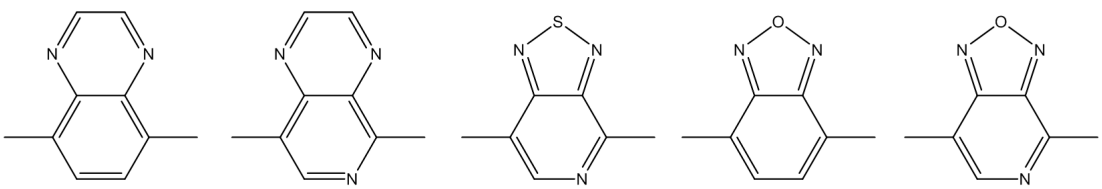

Fig. 3 Some electron-withdrawing moieties [53].

The ideal bandgap energy is determined by a balance between absorption gains and conversion losses. Although a reduced bandgap results in greater absorption of the available light, it also limits the ultimate level of the captured energy; an absorbed photon will relax to an energy level slightly less than the bandgap of the polymer. Although a polymer could absorb 90 % (70 %) of the sun's irradiance with a bandgap of 0.73 eV (1.24 eV), this would result in much energy loss in the conversion to useful current [48]. Therefore, in the interest of balancing these effects, an ideal bandgap for donor polymers in

PSCs is expected to be around 1.5 eV (with an absorption maximum around the maximum photon flux near 650–700 nm) [42,46,54].

A polymer with an appropriate bandgap and a wide spectral absorbance will maximize utilization of the solar spectrum [54]. Luckily, the amorphous nature of conjugated polymer films results in a wide range of effective conjugation lengths so that a wide band of wavelengths are absorbed. When this is combined with appropriate molecular design tailoring of the bandgap, a material acceptable for efficient PSCs can be created.

Tuning the HOMO and V_{oc}

Efficient PSCs must produce voltages commensurate with the energy that they absorb. Absorbed energy loses potential as it relaxes and is separated in the conversion process (Fig. 4). The maximum voltage that an organic solar cell can produce is limited by the minimum energy separation between the charges in a functioning device [55]. It has been observed that V_{oc} scales with the difference between the HOMO energy level of the donor polymer and the LUMO energy level of the acceptor molecule [34,42,56–59]. Aside from the recombination losses to V_{oc} mentioned earlier, this is a primary bottleneck for high PCE devices.

The most popular molecular design strategies for increasing V_{oc} involve increasing the donor HOMO–acceptor LUMO energy gap. By introducing pendant electron-withdrawing groups or by controlling polymer planarity the HOMO level can be modulated [17,18,26,27,31,33–35,46,59–61]. Since electronegative groups pull electron density into a localized area, they bind the electrons more tightly to, and stabilize the molecule, thus lowering the HOMO. By increasing the strength (electronegativity) of the withdrawing group, the HOMO can be sequentially lowered. Chen et al. were able to progres-

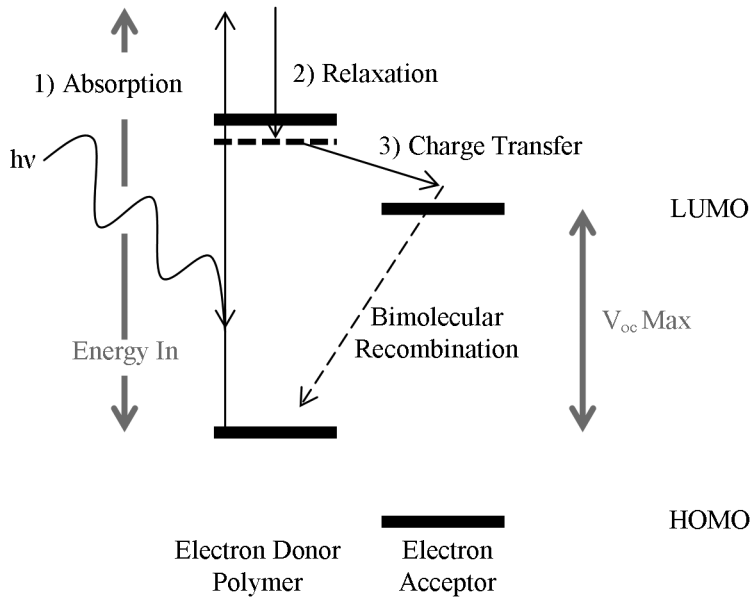

Fig. 4 The open circuit voltage and energy conversion losses. Energy conversion losses at zero current flow contribute to lowered V_{oc}. For instance, the absorption maximum of P3HT (530 nm) has the potential to create 2.34 eV, but relaxation to just below (due to the binding energy) its 1.9 eV bandgap reduces this prospective. Finally, charge-transfer and bimolecular recombination losses further reduce the voltage-creating capability to about 0.6 V in optimized devices.

sively lower the HOMO of a poly(thienothiophene-*alt*-benzodithiophene) from –5.01 to –5.12 to –5.22 eV by changing the pendant groups from an ester to a ketone and finally to a fluorine and ketone pair (Fig. 1g, 2,3,4) [34]. This resulted in an increase in PSC V_{oc} from 620 to 700 to 760 mV [34]. Some representative electron-withdrawing groups include diketone, benzothiadiazole (in the polymer backbone), ester, cyano, and fluorine [17,18,26,27,31,33–35,46,60]. The inclusion of these groups has led to HOMO levels as low as –5.73 eV (Fig. 1f), and V_{oc} values as high as 0.99 V [17,33]. These values are relative enhancements when compared to the HOMO (–4.9 eV) and V_{oc} (0.6 V) of the conventional material for PSCs, regioregular P3HT.

Polymer planarity and packing also play a role in determining the HOMO level. As the effective conjugation length increases in a polymer, the electrons are further delocalized and the HOMO level is raised. For instance, Trznadel et al. showed that increasing molecular weight led to a reduction in the oxidation potential of P3HT from 0.55 to 0.45 V; this corresponds to a HOMO level increase with increasing effective conjugation length [62]. This idea has been applied to modulate or reduce the HOMO to increase V_{oc}: Li et al. has varied the length and position of alkyl and alkoxy side-chains on a polymer (Fig. 1d) and noticed a modulation in the HOMO level between –5.4 and –5.6 eV [31]. Furthermore, Hou et al. created a polythiophene with a bulky 2-hexyldecyl chain on every third monomer (as compared to the hexyl side-chain on each P3HT monomer) resulting in a lowered HOMO level at –5.3 eV and an increased V_{oc} (0.82 V) [59]. While these HOMO level alterations could be attributed to changes in the population and electron-donating power of the side-chains, one cannot ignore the side-chain bulkiness. Bulky side-chains can reduce inter-chain packing and therefore the effective conjugation length.

Tuning the HOMO level of conjugated polymers has recently become the most popular method of increasing overall device efficiency [34,46]. However, much room for V_{oc} and PCE improvement remains; an absorbed photon has at least 1.7 eV (for that bandgap), yet most of the donor HOMO–acceptor LUMO energy gaps fall between 0.6 to 1.4 eV, furthermore, V_{oc} values are typically 0.1–0.3 eV lower than this [34,42,59,60]. Thus, more than half the potential voltage-creating capacity of an absorbed photon is lost in the conversion process (Fig. 4). Control over polymer packing, as mentioned earlier, and molecular orbital energy level tuning through molecular design can lead to further reductions in these losses and increases in device efficiency.

Stability of PSCs

Practical implementation of PSCs will require long device lifetimes (5–10 years at 8–16 % PCE by one estimate) in order to be cost-effective [63]. Although there have been reports of device lifetimes exceeding one year, there are many more reports of lifetimes closer to days or even just hours [4,7,19,37,64]. Unfortunately, there are relatively fewer publications about device lifetime enhancement (in comparison to efficiency enhancement or to understanding device physics) via molecular design, especially with regards to the polymer materials in champion efficiency devices. Nonetheless, we will briefly mention molecular design routes which can be used to enhance lifetime by combatting morphological instability and polymer degradation [4,19,36,37].

The performance of PSCs is sensitive to the phase-separated morphology of the donor–acceptor blend. Due to the exciton diffusion length limitations and the necessity for percolated conduction pathways in each phase, if the phase separation is not optimized, the device PCE suffers. Even when a device is fabricated with a near-optimum morphology, over time the morphology may overdevelop, especially for polymers with low glass-transition temperatures, leading to reduced lifetimes [37,65]. In order to combat this effect, some polymers have been designed with thermo-cleavable side-chains (at the junction between an ester and a tertiary alkyl chain, Fig. 1h). The side-chains initially impart the polymers with sufficient solubility for solution-state processing. Once the polymers are cast into a film, the side-chains are removed and the polymers have good thermal stability due to an increased glass-transition temperature [37]. Krebs et al. found that before cleavage, a PSC based on a polythiophene

with a cleavable side-chain degraded within 2 h; the analogous device with side-chains removed showed no appreciable degradation over the same time period [37]. Based on accelerated lifetime tests, they expect that a properly encapsulated device with a stable morphology would have a lifetime over two years [37].

Chemical degradation of conjugated polymers is a primary contributor to PSC device lifetime limitations. Studies where different encapsulation layers (which select particular ambient gasses) or different atmospheres are exposed to devices have shown that oxygen diffusion into the polymer and subsequent photo-oxidation lead to reduced device PCEs [4,5,19,36]. Energy transfer from the photo-excited polymer to oxygen can create a reactive singlet oxygen which will attack the polymer and oxidize the unsaturated backbone, thus leading to breakage of the conjugation (loss of conductivity) and device degradation [19,36]. While device encapsulation can greatly reduce these effects, molecular design can also enhance the oxidative stability of the polymers and devices [7,19,36]. The primary design route to protect against oxidation is to increase the oxidation potential of the polymer, or, in other words, to reduce the HOMO level. For instance, utilizing a polymer with a low HOMO level of –5.5 eV, Kim et al. found that no oxygen had attacked the conjugated backbone during a 40-h illumination/degradation test (whereas in P3HT, Fourier-transform infrared spectroscopy indicated that oxygen had bonded to the thiophene rings). Furthermore, this enhanced oxidative stability led to slight reductions in the device degradation rate. Molecular design can lower the HOMO level of the polymers as outlined in the previous section, and can therefore improve the PSC lifetime.

Morphology control

Morphology control and optimization in PSCs is a critical factor in determining the PCE. Appropriate phase separation that maintains connected pathways within each phase allows for efficient exciton separation and charge conduction, both critical steps in the power conversion process. Since this is such an important design factor, many reviews have been written on this subject [1,63,66–71]. As is detailed in the reviews, most schemes for controlling the micromorphology involve varying the polymer:PCBM mix ratio, using processing additives or appropriate solvents, or using post-processing steps such as solvent vapor or thermal annealing. Less commonly, the thermodynamics of phase separation are altered via molecular design [72–74]. For example, by modifying the surface energy of P3HT (with alcohol, bromo, methyl, or pentafluoro group chain termination) to better match that of PCBM, the mixing can be improved (Fig. 5) [72]. This mixing modification resulted in an increase in fill factor from 46 to 69 % and an improvement in PCE from 3.2 to 4.5 % [72]. Other more audacious schemes seek to take advan-

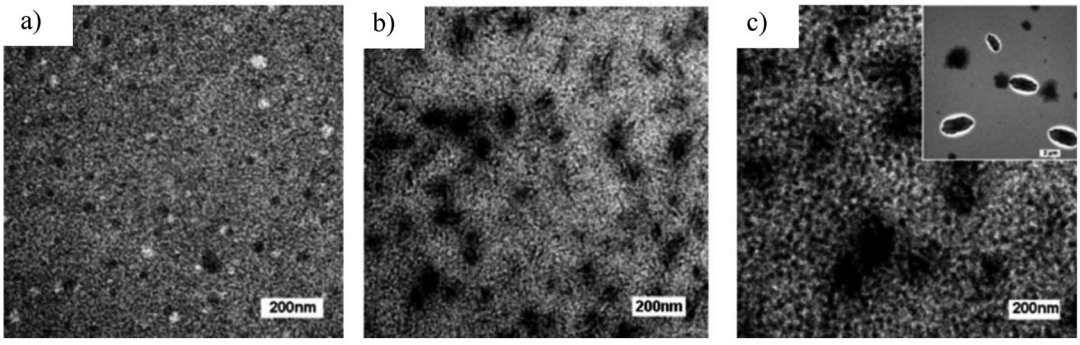

Fig. 5 Transmission electron microscopy (TEM) images showing improved mixing between end-modified P3HT and PCBM by changing the P3HT terminal group from (c) an alcohol, to (b) a bromine, and finally to (a) a pentafluoro group. The phase separation coarsens from images (a) to (c), and the inset of (c) shows a larger scale of separation. Adapted from [72].

tage of morphological self-assembly via block copolymer physics [73–75]. However, whether using the assembly of the block copolymers directly in the device or using the assembly as a template, these methods have not achieved great success, with PCEs below 1 % [73,74]. The importance of morphology in PSCs cannot be overstated; despite the previous lack of great success in molecular design of PSC blend morphology, these routes will likely continue to be explored in search of improved exciton and charge transport and improved PCE.

Novel polymers for PSCs

The aforementioned polymer design rules work to reduce losses in the energy conversion processes by increasing energy gathering, improving energy transport, and by optimizing molecular energy levels. Further improvements will continue to be made through synthesis of novel polymers that take advantage of the device operation physics. For instance, there has been some interest in replacing the fullerene electron acceptor molecules with n-type conducting polymers because they absorb the solar spectrum more strongly [76–82]. In order to function as an electron acceptor, a polymer must have a LUMO and HOMO lower than those of the donor material, and it must be able to conduct electrons. Polymer design strategies that assure electron-accepting character involve lowering the HOMO (and accompanying LUMO) level with electron-withdrawing groups similar to routes described in previous sections [77,81–83]. Although conjugated polymers have been shown to possess ambipolar conductivity, their electron mobility is typically one to three orders of magnitude smaller than their hole mobility, and is a performance-limiting property [80,82,84]. Molecular design routes for improving the electron mobility are also similar to those mentioned in earlier sections; charge carrier mobility is greater in more planar polymers, and planarity can be enhanced with large, rigid, fused ring moieties along the polymer backbone. By implementing almost comically large fused rings into the polymer backbone, the electron mobility has been enhanced to 10^{-1} to 10^{-2} $cm^2\ V^{-1}\ s^{-1}$ [83,85]. Despite these advances, because polymer–polymer blend solar cells are not widely popular, their PCEs are still limited to around 1.8 % [82].

Another category of novel polymers for PSCs seeks to increase the exciton diffusion length by using long-lived triplet excitons. As mentioned in the outset, short exciton diffusion lengths are a critical factor limiting the allowable morphologies in PSCs for effective energy conversion. Since the exciton diffusion length scales with the square root of the excitons lifetime, and since triplet excitons have lifetimes on the order of μs–ms, there has been interest in using phosphorescent materials to enhance PSCs [38,39,86–88]. Intersystem crossing to the triplet state is a forbidden transition, and special materials are required to facilitate its occurrence; molecular design routes to achieve triplet-generating polymers rely on the presence of heavy metal atoms like Pt and Pd [38,39,88]. For instance, by binding trace amounts of Pd onto a ladder-type poly(*para*-phenylene) (Fig. 1j), Arif et al. were able to increase the PCE by a factor of 10 (although only to 0.23 %) over the same polymer without heavy metals [39,88]. They attribute the improvement to the presence of long-lived (τ = 8.7 ms) triplet excitons, which enhance the current density (via improved exciton separation) [39]. Similarly, by including Pt atoms in the backbone of a thiophene acetylide polymer (Fig. 1i), Guo et al. were able to promote the formation of a triplet state (τ = 5.8 μs) in PSCs that contributed to charge separation and power conversion [38]. These devices show a good proof of concept that triplet states can enhance PSCs performance; the overall efficiencies of these devices could be improved by the molecular design routes discussed in earlier sections.

These two examples show how novel molecular design is being explored to improve PSCs. By taking advantage of the understanding of PSC operational physics, one can design novel materials that will pave the way for future improvements in molecular design.

OUTLOOK

The future of PSCs is very promising due to recent advances in molecular design and device PCE. A better understanding of the operational physics of PSCs through careful characterization has created a foundation for device improvement. Each step in the energy conversion process has potential for loss, but some steps are more critical than others. Absorption of sunlight places certain demands on the bandgap and thickness of the device. But efficient conversion to electricity requires optimized energy levels, morphology, and exciton and charge transport. Molecular design has afforded solutions to most of these problems, namely, the HOMO level has been lowered to enhance V_{oc} and the bandgap has been reduced to improve absorption of sunlight. Despite the improvements in PSC lifetime and PCE, there are still device-limiting material properties like exciton diffusion length and charge carrier mobility. Continuous development of the electron donor and acceptor materials (whether polymer or small molecule) will refine exciton and charge transport through tools like energy level and morphology tuning. It is also possible that novel design routes will become more successful or popular in the future. Different populations of excitons, such as triplet excitons, may be more thoroughly utilized in efficient PSCs. Or self-assembly may be utilized to control donor–acceptor phase separation and inter- and intramolecular packing and conformation. In any case, the flexibility afforded to conjugated polymers through intelligent molecular design will allow further development of these materials to take advantage of the peculiarities of the energy conversion process. Synthesis of new polymer materials will continue to lead to improvements in understanding PSC operation and improvements in PCE.

ACKNOWLEDGMENTS

This material is based on work supported as part of the Center for Solar and Thermal Energy Conversion, an Energy Frontier Research Center funded by the U.S. Department of Energy, Office of Science, Office of Basic Energy Sciences under Award Number DE-SC0000957.

REFERENCES

1. W. Cai, X. Gong, Y. Cao. *Sol. Energy Mater. Sol. Cells* **94**, 114 (2010).
2. H. J. Park, M. G. Kang, S. H. Ahn, L. J. Guo. *Adv. Energy Mater.* **22**, E247 (2010).
3. F. C. Krebs, T. Tromholt, M. Jørgensen. *Nanoscale* **2**, 873 (2010).
4. A. J. Medford, M. R. Lilliedal, M. Jørgensen, D. Aarø, H. Pakalski, J. Fyenbo, F. C. Krebs. *Opt. Expr*. **18**, A272 (2010).
5. F. C. Krebs, S. A. Gevorgyan, J. Alstrup. *J. Mater. Chem*. **19**, 5442 (2009).
6. New polymers push Solarmer's OPV efficiency to record 8.13 %, http://www.pv-tech.org/news/_a/new_polymers_push_solarmers_opv_efficiency_to_record_8.13/ (accessed July 2010).
7. J. A. Hauch, P. Schilinsky, S. A. Choulis, R. Childers, M. Biele, C. J. Brabec. *Sol. Energy Mater. Sol. Cells* **92**, 727 (2008).
8. I. W. Hwang, D. Moses, A. J. Heeger. *J. Phys. Chem. C* **112**, 4350 (2008).
9. R. A. Marsh, J. M. Hodgkiss, S. Albert-Seifried, R. H. Friend. *Nano Lett*. **10**, 923 (2010).
10. A. Pivrikas, N. S. Sariciftci, G. Juska, R. Osterbacka. *Prog. Photovolt.: Res. Appl.* **15**, 677 (2007).
11. P. E. Shaw, A. Ruseckas, I. D. W. Samuel. *Adv. Mater*. **20**, 3516 (2008).
12. K. M. Coakley, M. D. McGehee. *Chem. Mater*. **16**, 4533 (2004).
13. G. Yu, J. Gao, J. C. Hummelen, F. Wudl, A. J. Heeger. *Science* **270**, 1789 (1995).
14. Y. Li, Y. Zou. *Adv. Mater*. **20**, 2952 (2008).
15. H. A. Becerril, N. Miyaki, M. L. Tang, R. Mondal, Y. S. Sun, A. C. Mayer, J. E. Parmer, M. D. McGehee, Z. Bao. *J. Mater. Chem*. **19**, 591 (2009).
16. M. S. Kim, B. G. Kim, J. Kim. *Appl. Mater. Interfaces* **1**, 1264 (2009).

17. F. Huang, K. S. Chen, H. L. Yip, S. K. Hau, O. Acton, Y. Zhang, J. Luo, A. K. Y. Jen. *J. Am. Chem. Soc.* **131**, 13886 (2009).
18. L. Huo, J. Hou, S. Zhang, H. Y. Chen, Y. Yang. *Angew. Chem*. **122**, 1542 (2010).
19. S. H. Kim, I. W. Hwang, Y. Jin, S. Song, J. Moon, H. Suh, K. Lee. *Sol. Energy Mater. Sol. Cells* (2010). doi:10.1016/j.solmat.2009.12.013
20. Y. Li, Y. Zou. *Adv. Mater*. **20**, 2952 (2008).
21. Y. Liang, Y. Wu, D. Feng, S. T. Tsai, H. J. Son, G. Li, L. Yu. *J. Am. Chem. Soc.* **131**, 56 (2009).
22. B. J. Schwartz. *Annu. Rev. Phys. Chem*. **54**, 141 (2003).
23. J. Lee, H. J. Kim, T. Chen, K. Lee, K. S. Kim, S. C. Glotzer, J. Kim, N. A. Kotov. *J. Phys. Chem. C* **113**, 109 (2009).
24. Y. Kim, S. Cook, S. Tuladhar, S. A. Choulis, J. Nelson, J. R. Durrant, D. C. Bradley, M. Giles, I. McCulloch, C. S. Ha, M. Ree. *Nat. Mater.* **5**, 197 (2006).
25. B. Lim, K. J. Baeg, H. G. Jeong, J. Jo, H. Kim, J.-W. Park, Y. Y. Noh, D. Vak, J. H. Park, J.-W. Park, D. Y. Kim. *Adv. Mater.* **21**, 2808 (2009).
26. R. Qin, W. Li, C. Li, C. Du, C. Veit, H. F. Schleiermacher, M. Andersson, Z. Bo, Z. Liu, O. Inganas, U. Wuerfel, F. Zhang. *J. Am. Chem. Soc.* **131**, 14612 (2009).
27. S. Xiao, A. C. Stuart, S. Liu, W. You. *Appl. Mater. Interfaces* **1**, 1613 (2009).
28. C. Y. Yu, B. T. Ko, C. Ting, C. P. Chen. *Sol. Energy Mater. Sol. Cells* **93**, 6113 (2009).
29. P. J. Brown, D. S. Thomas, A. Kohler, J. S. Wilson, J. S. Kim, C. M. Ramsdale, H. Sirringhaus, R. H. Friend. *Phys. Rev. B* **67**, 064203 (2003).
30. I. McCulloch, M. Heeney, C. Bailer, K. Genevicius, I. MacDonald, M. Shkunov, D. Sparrowe, S. Tierney, R. Wagner, W. Zhang, M. L. Chabinyc, R. J. Kline, M. D. McGehee, M. F. Toney. *Nat. Mater.* **5**, 328 (2006).
31. W. Li, R. Qin, Y. Zhou, M. Andersson, F. Li, C. Zhang, B. Li, Z. Bo, F. Zhang. *Polymer* **51**, 3031 (2010).
32. D. Mühlbacher, M. Scharber, M. Morana, Z. Zhu, D. Waller, R. Gaudiana, C. Brabec. *Adv. Mater*. **18**, 2884 (2006).
33. K. Colladet, S. Fourier, T. J. Cleij, L. Lutsen, J. Gelan, D. Vanderzande, L. H. Nguyen, H. Neugebauer, S. Sariciftci, A. Aguirre, G. Janssen, E. Goovaerts. *Macromolecules* **40**, 65 (2007).
34. H. Y. Chen, J. Kou, S. Zhang, Y. Liang, G. Yang, Y. Yang, L. Yu, Y. Wu, G. Li. *Nat. Phot*. **3**, 649 (2009).
35. Y. Zou, A. Najari, P. Berrouard, S. Beaupré, B. R. Aïch, Y. Tao, M. Leclerc. *J. Am. Chem. Soc*. **132**, 5330 (2010).
36. M. Jørgensen, K. Norrman, F. C. Krebs. *Sol. Energy Mater. Sol. Cells* **92**, 686 (2008).
37. F. C. Krebs, H. Spanggard. *Chem. Mater*. **17**, 5235 (2005).
38. F. Guo, Y. G. Kim, J. R. Reynolds, K. S. Schanze. *Chem. Commun.* **17**, 1887 (2006).
39. M. Arif, K. Yang, L. Li, P. Yu, S. Guha, S. Gangopadhyay, M. Forster, U. Scherf. *Appl. Phys. Lett*. **94**, 063307 (2009).
40. O. Bolton, J. Kim. *J. Mater. Chem*. **17**, 1981 (2007).
41. Z. Zhu, D. Mühlbacher, M. Morana, M. Koppe, M. C. Scharber, D. Waller, G. Dennler, C. J. Brabec. "Design rules for efficient organic solar cells", in *High-Efficient Low-Cost Photovoltaics*, Vol. 140, pp. 195–222, Springer, Berlin/Heidelberg (2009).
42. M. C. Scharber, D. Mühlbacher, M. Koppe, P. Denk, C. Waldauf, A. J. Heeger, C. J. Brabec. *Adv. Mater*. **18**, 789 (2006).
43. K. Vandewal, K. Tvingstedt, A. Gadisa, O. Inganas, J. V. Manca. *Nat. Mater*. **8**, 904 (2009).
44. M. D. Perez, C. Borek, S. R. Forrest, M. E. Thompson. *J. Am. Chem. Soc.* **131**, 9281 (2009).
45. Y. Zhang, S. K. Hau, H. L. Yip, Y. Sun, O. Acton, A. K. Y. Jen. *Chem. Mater.* **22**, 2696 (2010).
46. Y. Liang, Z. Xu, J. Xia, S. T. Tsai, Y. Wu, G. Li, C. Ray, L. Yu. *Adv. Mater*. **22**, E135 (2010).

47. M. Svensson, F. Zhang, S. C. Veenstra, W. J. H. Verhees, J. C. Hummelen, J. M. Kroon, O. Inganas, M. R. Andersson. *Adv. Mater*. **15**, 988 (2003).
48. C. A. Gueymard. *Sol. Energy* **76**, 423 (2004).
49. C. Winder, N. S. Sariciftci. *J. Mater. Chem.* **14**, 1077 (2004).
50. J. Roncali. *Chem. Rev.* **97**, 173 (1997).
51. E. E. Havinga, W. Hoeve, H. Wynberg. *Polym. Bull.* **29**, 119 (1992).
52. H. Zhou, L. Yang, S. Stoneking, W. You. *Appl. Mater. Interfaces* **2**, 1377 (2010).
53. N. Blouin, A. Michaud, D. Gendron, S. Wakim, E. Blair, R. Neagu-Plesu, M. Belletête, G. Durocher, Y. Tao, M. Leclerc. *J. Am. Chem. Soc.* **130**, 732 (2008).
54. F. Shi, G. Fang, F. Liang, L. Wang, Z. Mu, X. Zhang, Z. Xie, Z. Su. *Eur. Polym. J.* **46**, 1770 (2010).
55. B. P. Rand, D. P. Burk, S. R. Forrest. *Phys. Rev. B* **75**, 115327 (2007).
56. A. Gadisa, M. Svensson, M. R. Andersson, O. Inganas. *Appl. Phys. Lett.* **84**, 1609 (2004).
57. T. Yamanari, T. Taima, J. Sakai, K. Saito. *Sol. Energy Mater. Sol. Cells* **93**, 759 (2009).
58. V. D. Mihailetchi, P. W. M. Blom, J. C. Hummelen, M. T. Rispens. *J. Appl. Phys.* **94**, 6849 (2003).
59. J. Hou, T. L. Chen, S. Zhang, L. Huo, S. Sista, Y. Yang. *Macromolecules* **42**, 9217 (2009).
60. S. Berson, S. Cecioni, M. Billon, Y. Kervella, R. de Bettignies, S. Bailly, S. Guillerez. *Sol. Energy Mater. Sol. Cells* **94**, 699 (2010).
61. E. Wang, L. Wang, L. Lan, C. Luo, W. Zhuang, J. Peng, Y. Cao. *Appl. Phys. Lett.* **92**, 033307 (2008).
62. M. Trznadel, A. Pron, M. Zagorska, R. Chrzaszcz, J. Pielichowski. *Macromolecules* **31**, 5051 (1998).
63. G. Dennler, M. C. Scharber, C. J. Brabec. *Adv. Mater.* **21**, 1323 (2009).
64. S. H. Park, A. Roy, S. Beaupré, S. Cho, N. Coates, J. S. Moon, D. Moses, M. Leclerc, K. Lee, A. J. Heeger. *Nat. Phot.* **3**, 297 (2009).
65. X. Yang, J. K. J. van Duren, R. A. J. Janssen, M. A. J. Michels, J. Loos. *Macromolecules* **37**, 2151 (2004).
66. H. Hoppe, N. S. Sariciftci. *J. Mater. Chem*. **16**, 45 (2006).
67. A. C. Mayer, S. R. Scully, B. E. Hardin, M. W. Rowell, M. D. McGehee. *Materials Today* **10**, 28 (2007).
68. S. Günes, H. Neugebauer, N. S. Sariciftci. *Chem. Rev.* **107**, 1324 (2007).
69. R. Giridharagopal, D. S. Ginger. *J. Phys. Chem. Lett*. **1**, 1160 (2010).
70. X. Yang, J. Loos. *Macromolecules* **40**, 1353 (2007).
71. L. Chen, Z. Hong, G. Li, Y. Yang. *Adv. Mater.* **21**, 1434 (2009).
72. J. S. Kim, Y. Lee, J. H. Lee, J. H. Park, J. K. Kim, K. Cho. *Adv. Mater*. **22**, 1355 (2010).
73. S. S. Sun, C. Zhang, A. Ledbetter, S. Choi, K. Seo, C. E. Bonner, M. Drees, N. S. Sariciftci. *Appl. Phys. Lett*. **90**, 043117 (2007).
74. R. Q. Png, P. J. Chia, J. C. Tang, B. Liu, S. Sivaramakrishnan, M. Zhou, S. H. Khong, H. S. O. Chan, J. H. Burroughes, L. L. Chua, R. H. Friend, P. K. H. Ho. *Nat. Mater*. **9**, 152 (2010).
75. F. S. Bates, G. H. Fredrickson. *Phys. Today* **52**, 32 (1999).
76. S. A. Jenekhe, S. Yi. *Appl. Phys. Lett*. **77**, 2635 (2000).
77. M. M. Mandoc, W. Veurman, J. Sweelssen, M. M. Koetse, P. W. M. Blom. *Appl. Phys. Lett*. **91**, 073518 (2007).
78. C. R. McNeill, N. C. Greenham. *Adv. Mater.* **21**, 3840 (2009).
79. M. M. Koetse, J. Sweelssen, K. T. Hoekerd, H. F. M. Schoo, S. C. Veenstra, J. M. Kroon, X. Yang, J. Loos. *Appl. Phys. Lett*. **88**, 083504 (2006).
80. C. R. McNeill, A. Abrusci, J. Zaumseil, R. Wilson, M. J. McKiernan, J. H. Burroughes, J. J. M. Halls, N. C. Greenham, R. H. Friend. *Appl. Phys. Lett*. **90**, 193506 (2007).
81. C. R. McNeill, J. J. M. Halls, R. Wilson, G. L. Whiting, S. Berkebile, M. G. Ramsey, R. H. Friend, N. C. Greenham. *Adv. Funct. Mater*. **18**, 2309 (2008).

82. S. C. Veenstra, J. Loos, J. M. Kroon. *Prog. Photovolt.: Res. Appl.* **15**, 727 (2007).
83. X. Zhan, Z. Tan, B. Domercq, Z. An, X. Zhang, S. Barlow, Y. Li, D. Zhu, B. Kippelen, S. R. Marder. *J. Am. Chem. Soc.* **129**, 7246 (2007).
84. R. Steyrleuthner, S. Bange, D. Neher. *J. Appl. Phys.* **105**, 064509 (2009).
85. H. Yan, Z. Chen, Y. Zhang, C. Newman, J. R. Quinn, F. Dotz, M. Kastler, A. Facchetti. *Nature* **457**, 679 (2009).
86. B. P. Rand, S. Schols, D. Cheyns, H. Gommans, C. Girotto, J. Genoe, P. Heremans, J. Poortmans. *Org. Elec.* **10**, 1015 (2009).
87. B. P. Rand, C. Girotto, A. Mityashin, A. Hadipour, J. Genoe, P. Heremans. *Appl. Phys. Lett.* **95**, 173304 (2009).
88. K. Yang, M. Arif, M. Forster, U. Scherf, S. Guha. *Synth. Met*. **159**, 2338 (2009).

